A BAYESIAN MIXED MULTISTATE OPEN-ROBUST DESIGN MARK-RECAPTURE MODEL TO ESTIMATE HETEROGENEITY IN TRANSITION RATES IN AN IMPERFECTLY DETECTED SYSTEM

By

Janelle J. Badger, B.S.

A Project Submitted in Partial Fulfillment of the Requirements

for the Degree of

Master of Science

in

Statistics

University of Alaska Fairbanks

December 2020

Dr. Julie McIntyre, Committee Chair
Dr. Ron Barry, Committee Member
Dr. Scott Goddard, Committee Member
Dr. Greg Breed, Committee Member
Dr. Leah Berman, Chair
Department of Mathematics & Statistics

Abstract

Multistate mark-recapture models have long been used to assess ecological and demographic parameters such as survival, phenology, and breeding rates by estimating transition rates among a series of latent or observable states. Here, we introduce a Bayesian mixed multistate open robust design mark recapture model (MSORD), with random intercepts and slopes to explore individual heterogeneity in transition rates and individual responses to covariates. We fit this model to simulated data sets to test whether the model could accurately and precisely estimate five parameters, set to known values a priori, under varying sampling schemes. To assess the behavior of the model integrated across replicate fits, we employed a two-stage hierarchical model fitting algorithm for each of the simulations. The majority of model fits showed no sign of inadequate convergence according to our metrics, with 81.25% of replicate posteriors for parameters of interest having general agreement among chains ($\hat{r} < 1.1$). Estimates of posterior distributions for mean transition rates and standard deviation in random intercepts were generally well-defined. However, we found that models estimated the standard deviation in random slopes and the correlation among random effects relatively poorly, especially in simulations with low power to detect individuals (e.g. low detection rates, study duration, or secondary samples). We also apply this model to a dataset of 200 female grey seals breeding on Sable Island from 1985-2018 to estimate individual heterogeneity in reproductive rate and response to near-exponential population growth. The Bayesian MSORD estimated substantial variation among individuals in both mean transition rates and responses to population size. The correlation among effects trended positively, indicating that females with high reproductive performance (more positive intercept) were also more likely to respond better to population growth (more positive slope) and vice versa. Though our simulation results lend confidence to analyses using this method on well developed datasets on highly observable systems, we caution the use of this framework in sparse data situations.

Introduction

Capture-mark-recapture methods (CMR) are basic tools for estimating demographic parameters (e.g. survival probability, reproductive rates) in populations subject to imperfect detection. An important development for CMR models was the recognition that many are a specific type of a "multistate" model (Lebreton et al. 1999, Lebreton and Pradel 2002). Multistate methods are used to model processes in which an animal stochastically moves among a series of latent or observable states, such as breeding states (breeding or non-breeding), physiological states (e.g. alive or dead, disease status) or even home range cores (Arnason 1972, Lebreton and Pradel 2002,Gimenez et al. 2007,Boulanger et al. 2013, Breed et al. 2016, Eisaguirre *in revision*, Johns et al. 2018). State-space models can disentangle population processes by distinguishing this underlying "state" in a multistate process, e.g. the survival or breeding state, from their "observation" process, i.e. the detectability (Gimenez et al. 2007). The state equation of the state-space formulation describes the true development of the states, describing the state of an individual at time $t+1$ given its state at time t, then the observation equation maps the true state at time t on to what is observed. This connection between state-space modeling and multistate modeling allows simplification of complex likelihoods into latent-state transitions and conditional Bernoulli observations (Lebreton et al. 2009).

For iteroparous breeding animals, this framework has been particularly useful in estimating the cost of reproduction (e.g. Beauplet et al. 2006, Hernández-Matías et al. 2011, Chambert et al. 2013, Stoelting et al. 2015, Johns et al. 2018). A common approach is to determine whether breeding at time t negatively affects an individual's probability of surviving from time t to $t+1$ or its probability of breeding at time $t+1$. A cost of reproduction may then be revealed as a higher probability of transition into a reproductive state in year $t+1$ following a nonreproductive state in year t. Because non-breeders often use different habitats than breeders (Bull and Shine 1979), when estimating transitions among breeding states, we are often also estimating transitions into and out of the study area (Kendall and Nichols 2002). The temporary movement out of the study area is a behavior termed *temporary emigration*.

Temporary emigration is inherently confounded with detection error in CMR modeling, as an individual could be not sighted in a given sample because they were unavailable for recapture (i.e. not breeding, temporarily emigrated) or, despite the fact they were available for capture, they remained undetected in sampling. Currently, sampling under Pollock's robust design (Pollock 1982) is the best way of obtaining unbiased estimates of demographic rates in systems with temporary emigration from the study area (Kendall et al. 2019). The multistate robust design modeling framework (MSRD) incorporates multiple capture occasions (secondary samples) per period of interest (usually seasons or years, primary samples) to exploit within-and-between period information simultaneously to obtain more robust estimates of survival, temporary emigration, detection, and abundance (Kendall et al. 1997). Schwarz and Stobo (1997) modified this approach to relax assumptions of closed populations, termed the multistate open robust design (MSORD). These methods are more complex and data-hungry than typical CMR methods, but offer more precise and accurate parameter estimates (Kendall et al. 1997, Schwarz and Stobo 1997, Kendall and Bjorkland 2001, Boys et al. 2019, Kendall et al. 2019).

MSRD and MSORD models are typically fit within a frequentist framework (i.e. program MARK) but have more recently been adapted to Bayesian methods due to inherent estimation challenges of temporary emigration (Kendall et al. 2019). Advances in both estimation techniques have provided incorporation of random intercepts to account for individual heterogeneity in MSRD models, almost exclusively in detection probabilities (Rankin et al. 2016, Boys et al. 2019). However, individual heterogeneity in transition rates is an equally important factor in precise and accurate parameter estimates (Gimenez et al. 2017), and is of special interest when investigating costs of reproduction (Chambert et al. 2013). Here, we introduce a Bayesian MSORD with random intercepts and slopes to explore individual heterogeneity in transition rates and individual responses to covariates.

Statistical Methods

Notation used

We consider a population of females that move through two states: breeder or nonbreeder

(temporary migrant), where individuals are only detected in the breeding state and are necessarily undetected in a nonbreeding state during the breeding season. Detections occur according to a nested sampling design with $t \in [1,...,T]$ primary periods and $s \in [1,...,S_t]$ secondary periods within each primary period. The number of secondary periods may vary per primary period, and S_{max} is the maximum number of all S_t. We condition the modeling framework between each individual i's first detection f_i and last detection l_i and thus survival is known and not estimated here.

Data

n is the total number of uniquely marked animals encountered during the entire study

$\boldsymbol{Y}^{(n \times S_{max} \times T)}$ is the array of capture histories over all observed individuals n in T primary periods and S_{max} secondary periods, with individual elements $y_{i,s,t} = 1$ if individual i was encountered in secondary period s within primary period t or $y_{i,s,t} = 0$ if individual i was not encountered in secondary period s within primary period t.

C_t is the value of a time-varying covariate at time t for which there is an individual random slope.

f_i is a vector of length n which indicates the first primary period $f_i \in [1,...,T]$ in which individual i was sighted.

l_i is a vector of length n which indicates the last primary period $l_i \in [1,...,T]$ in which individual i was sighted.

Estimated parameters or latent variables

$\boldsymbol{Z}^{(n \times T)}$ is a matrix of latent states $z_{i,t} \in \{0,1\}$ that indicate the breeding state of individual i during primary period t, where the value is assigned to represent states $\{$*not breeding, breeding*$\}$.

$M^{(n \times S_{max} \times T)}$ is an array of latent states where $m_{i,s,t} \in \{1,2,3\}$ indicates individual i as being in one of three states at secondary sample s during primary period t, where values are assigned to represent states $\{$*not yet arrived, at study area, departed*$\}$.

$p_{s,t}$ is the probability of detecting a marked animal in secondary period s within primary period t.

γ is the probability that a marked animal will arrive onsite during a given secondary period.

ϕ is the probability that a marked animal remains onsite during a given secondary period, i.e. the residence probability.

$S_{i,t}$ is the number of secondary periods $S_{i,t} \in [1,...,S_t]$ individual i is onsite during year t.

$\psi_{i,t}^{k1}$ is the probability of reproduction, defined as the probability that individual i is in a breeding state in year t given she was in state k in year $t-1$. Complementary transition rates (1- $\psi_{i,t}^{k1}$) represent the probability that individual i is a nonbreeder in year t.

$\mu_{i,z_{t-1}}$ is the effect of the previous state $z_{i,t-1}$ on the reproductive rate, or probability of transition into breeding state $z_{i,t} = 1$.

η is the estimated fixed effect of covariate C_t on response variable ψ^{k1}.

α_i is the fitted estimate for the random intercept $\boldsymbol{\alpha}$ for individual i, where $\alpha_i \sim N(0, \sigma_\alpha^2)$.

β_i is the fitted estimate for the random slope $\boldsymbol{\beta}$ for individual i, where $\beta_i \sim N(0, \sigma_\beta^2)$.

$\rho(\boldsymbol{\alpha}, \boldsymbol{\beta})$ is the estimated correlation between random effects $\boldsymbol{\alpha}$ and $\boldsymbol{\beta}$.

θ_t is the random year effect $\boldsymbol{\theta}$, where $\theta_i \sim N(0, \sigma_\theta)$

Model Specification

We use a multistate open robust design mark recapture model to estimate transition rates among reproductive states, and generalized linear random effect models to estimate individual random effect variances. The likelihood for the model can be written as:

$z_{i,f_i} = 1$

$z_{i,t} \sim \text{Bern}(\psi^{k1}_{i,t-1})$ for t $\in \{f_i + 1, ..., l_i\}$

$E[\text{logit}(\psi^{k1}_{i,t})] = \mu_{i,z_{t-1}} + \eta \cdot C_t + \alpha_i + \beta_i \cdot C_t + \theta_t$

$m_{i,1,t}|z_{i,t} \sim \text{Cat}[z_{i,t} \cdot \gamma]$, where $\gamma = \{1-\gamma, \gamma, 0\}$

$m_{i,s,t}|z_{i,t}, m_{i,s-1,t} \sim \text{Cat}[z_{i,t} \cdot \{(\text{I}(m_{i,s-1,t} = 2) \cdot \phi + \gamma \cdot \prod_{j=1}^{s} \text{I}(m_{i,j,t} = 1)\}]$ for s $\in \{2..., s_t\}$

$y_{i,s,t}|m_{i,s,t} \sim \text{Bern}[\text{I}(m_{i,s,t} = 2) \cdot p_{s,t}]$

Between an individual's first and last primary sightings (f_i to l_i) during the period of study, we model their sighting history as a Markov chain in which the individual transitions between breeding ($z_{i,t} = 1$) and nonbreeding states ($z_{i,t} = 0$), termed the z state process. Individuals are necessarily breeding upon their first sighting at the breeding season, so $z_{i,f_i} = 1$. Reproductive rate is then defined here as the probability of transition ψ^{k1} from any state k such that $z_{i,t} \in \{0,1\}$ to the breeding state, $z_{i,t} = 1$. Reproductive rate can then be modeled as a function of many covariates, but here we simply model this parameter as a function of random effects: individual intercepts α, individual slopes with a covariate β, random time effect θ and error term ϵ. Individual random effects α and β are drawn from a multivariate normal distribution $N_2(0, \Sigma)$, where $\Sigma = \begin{bmatrix} \sigma^2_\alpha & \rho(\alpha,\beta) \cdot \sigma_\alpha \cdot \sigma_\beta \\ \rho(\alpha,\beta) \cdot \sigma_\alpha \cdot \sigma_\beta & \sigma^2_\beta \end{bmatrix}$. An individual's state transition from primary period t to primary period $t+1$ is modeled as a probabilistic draw with probability of transition ψ^{ks} from state k to state s. Here, we assume two states and a Bernoulli process, but this framework could be easily modified to accommodate more states (e.g. breeding at site A, breeding at site B, not breeding), by using a Categorical process, e.g. $z_{i,t} \sim \text{Cat}(\psi^{ks}_{i,t-1})$ (Kéry and Schaub 2012, Kendall et al. 2019).

Primary periods are governed by the multi-state process z of individuals switching between breeding states, as described above (Figure 1). We assume the primary period probability of detection p_t may vary among primary periods, but probability of detection for secondary samples $p_{s,t}$ is constant over the course of a primary period and across individuals. The probability that

individuals are detected, given they are onsite, is estimated from the secondary samples. Secondary samples within a primary period are modeled using a multistate formulation of the full-capture open population Jolly-Seber model (Jolly 1965, Seber 1965). Individuals may be in three states: not yet arrived at the study area $m_{i,s,t} = 1$, at the study area $m_{i,s,t} = 2$, or departed from the study area $m_{i,s,t} = 3$ (Figure 1). Similar to the primary period state process z, the latent state process m is not known, but drawn from a probability distribution. For example, if individual i is at the study area at secondary sample s in primary period t so $m_{i,s,t} = 2$, the observation for each secondary period is a simple Bernoulli process with detection probability $p_{s,t}$, i.e. $\text{P}(y_{i,s,t}|m_{i,s,t} = 2) = \text{Bern}(p_{s,t})$. Then, the probability that the individual is observed in at least one secondary sample s in a primary period t is estimated by $\hat{p}_t = 1 - \prod_{s=1}^{S_{i,t}}(1 - p_{s,t})$. Individuals move from not yet arrived at the study area ($m_{i,s,t} = 1$) to at the study area ($m_{i,s,t} = 2$) based on the entry probability γ and remain in the study area with the residence probability ϕ. The number of secondary periods an individual is available for capture (on site) $S_{i,t}$ is then drawn from a Geometric(1-$\phi_{i,t}$) distribution, and so individuals move from the study area to departed from study area ($m_{i,s,t} = 3$) based on the departure probability (1-ϕ).

Parameter Estimation

We fit this model using a publicly available Bayesian software program JAGS 4.2.0 (Plummer 2003) within the R statistical environment using the interface `rjags` (Plummer 2018). Priors for state-specific means μ_0 and μ_1 were given uninformative Beta(1,1) priors. The standard deviation of the random year effect θ_t was given a Unif(0,5) prior. For the recapture model, we used an uninformative Beta(1,1) prior for entry probability γ, detection probability $p_{s,t}$, and residence probability ϕ.

Individual random effects are drawn from a multivariate normal distribution with mean vector 0 and variance-covariance matrix Σ (as described above), and estimation is accomplished using the `dmnorm.vcov` function within JAGS, which tosses out non-positive definite proposal variance-covariance matrices. Standard deviations of the random effects, σ_α and σ_β were given Unif(0,5) priors, and we used a Unif(-1,1) prior for the correlation among individual effects $\rho(\alpha, \beta)$. Alternatively, users

may take advantage the conjugacy of the multivariate normal distribution and the Inverse Wishart, such that $\Sigma \sim \text{Inverse Wishart}(\nu_0, S_0^{-1})$, where ν_0 represents degrees of freedom and S_0 is some scale matrix. However, though this approach is common in Bayesian mixed-effects regression models, it can have problems constraining the combination of covariances resulting in accidentally informative priors on the standard deviations of the random effects, biasing estimates (Riecke et al. 2019).

Markov chain Monte Carlo (MCMC) methods were used to sample the posterior distributions of the parameters of interest. We ran three chains in parallel using package `dclone` (Solymos 2010) with different sets of initial values. The first 10,000 MCMC samples were discarded, known as the burn-in period, after which chains ran for 100,000 iterations, and 1,000 samples from each were retained for inference.

Simulation Design & Implementation

We fit this model to simulated data sets to test whether the model could accurately and precisely estimate five parameters, set to known values a priori, under varying sampling schemes. These parameters include mean transition rates into the breeding state from breeding (μ_1) and nonbreeding (μ_0) states, random effect standard deviations σ_α and σ_β, and the correlation among random effects $\rho(\boldsymbol{\alpha}, \boldsymbol{\beta})$. We consider five, two-level variables in a 2^5 factorial design that influence the ability of the model to estimate parameters for a total of 32 sets of conditions (Table 1): sample size (low, n = 50; high, n =100), study duration (low, T = 10; high, T = 20), number of secondary samples (low, S_{max} =3; high, S_{max} = 7), secondary sample detection error (low, $p_{s,t}$ = 0.7; high, $p_{s,t}$ = 0.3), and level of heterogeneity among individuals (low, σ^2 = 0.1; high, σ^2 = 0.5). We simulated a decreasing continuous covariate C_t, standardized, for the random slope $\boldsymbol{\beta}$. We ran the Bayesian MSORD for each combination of these conditions, termed hereafter *simulations*, replicated for 50 such data sets (termed hereafter *replicates*), resulting in 1600 model fits.

We employ a two-stage model fitting algorithm for each of the 32 simulations: the first stage, running all 50 replicates, then the second, using a simplified MCMC algorithm to fit a full hierarchical model using the output from the first stage as proposal distributions. This technique has been used

in hierarchical state-space animal movement models to make population-level inference on latent parameters or processes (Hooten et al. 2016). Here, we use the approach to aid in interpreting results, integrating across replicates to capture coverage of the model for each simulation.

This approach will yield two modes of observation for the behavior of this model: posterior distributions from 50 individual replicates per simulation, which we will refer to as *replicate posteriors*, and posterior distributions from one hierarchical MCMC per simulation (integrating across the 50 replicates), which we will refer to hereafter as the *hierarchical posteriors*. Performance of the model under these varying simulations is assessed using three metrics: the proportion of replicate fits for which the 50% highest posterior density interval (referred to hereafter as $_{50}$HPD) contains the true value, the proportion of $\hat{r}$ (ratio of the average variance of draws within each chain to the variance of the pooled draws across chains, value greater than 1 indicating lack of convergence) that are less than 1.1, and bias of hierarchical posterior means.

Results

The majority of model fits showed no sign of inadequate convergence according to our metrics, with 81.25% of replicate posteriors for parameters of interest having general agreement among chains ($\hat{r} < 1.1$, Table 2).

The model performed well at estimating transition rates μ_1 and μ_0, with $_{50}$HPDs of replicates covering the true value 89.3% and 90.9% of the time, respectively. Similarly, $_{50}$HPDs of hierarchical posteriors contained the true value 96% and 94.3% of the 32 simulations (Fig. 2). Mean bias in hierarchical posteriors (difference between true value and model-estimated posterior mean) was quite low, but indicate estimates may be slightly underestimated for μ_1 (Fig.3). Poorest performers were models fit to simulated data sets with high heterogeneity among individuals ($h = 0.5$) but low sample size and/or time series length.

Standard deviation among individuals in intercepts (σ_α) was estimated well, with 86.5% of $_{50}$HPDs including the true value, but estimation of standard deviation in individual responses to a continuous covariate (σ_β) performed relatively poorly across replicate fits, with only 46.4% of $_{50}$HPDs including the true value (Fig. 2). Hierarchical posterior mean bias was lower in σ_β than

σ_α, but distinctly more variable (Fig. 3). Models fit to data sets with a longer time series performed substantially better than short time series, especially when coupled with high detection rates and/or more secondary samples (Figure 5). In simulations with low heterogeneity among individuals, without proper detection or time series length, the models seemed unable to distinguish individual slopes and individual slope β_i posteriors tended toward zero. Models fit to datasets with a low sample size tended to underestimate heterogeneity among individuals, σ_α.

In 92.4% of replicate fits, the $_{50}$HPDs of the correlation among individual effects, $\rho(\alpha, \beta)$, contained the true value. However, though replicate posterior modes for $\rho(\alpha, \beta)$ are distinct and near the true value, distributions often appeared quite wide even in the best fits (Fig. 2), and so the high coverage rate may be an artifact of a relatively uninformed distribution. Mean bias in hierarchical model fits showed that this parameter can be biased high, but bias is quite variable across simulations (Fig. 3).

Application to grey seal reproductive heterogeneity

We demonstrate this model via application to a long-term mark-recapture data set to explore individual reproductive heterogeneity in female grey seals (*Halichoerus grypus*) that breed on Sable Island, Nova Scotia (43.93N, 59.91W). Our sample of 200 females were marked as pups shortly after weaning in 1985, 1986, 1987, and 1989 with unique alpha-numeric brands. These permanent brands allowed reliable identification of individuals over the course of their lives. Each week during their breeding season (early December - early February), researchers systematically search the island for branded females, resulting in 5-7 censuses per year. Individual sighting histories were collected from age at first reproduction (first sighting in breeding colony, typically around 5 years of age) until death (or 2018 for animals still living). Sighting histories of individuals were scored as a 0 (not sighted) or 1 (sighted) for each week (secondary sample) in each breeding season (primary sample) from 1985-2018. Females sighted in only one breeding season were omitted from this analysis to ensure that they had in fact recruited to the Sable Island breeding population and we have adequate data to estimate individual responses.

This population has undergone extraordinary growth over the past half century, with pup

production on the island increasing at nearly exponential rates (13% per year) from 1960s - 1997 and a reduced rate (4% per year) through 2016 (den Heyer et al. 2017). Ecological theory suggests that increases in population density may impose per capita resource scarcity and negatively affect vital rates, such as fecundity (Eberhardt and Siniff 1977, McLoughlin et al. 2006, Zachar and Neiman 2013). However, there is no evidence to suggest population-wide resource limitation–after the collapse of the cod fishery in the early 1990s, there was actually an increase in the pelagic forage fish on the Scotian Shelf (Frank et al. 2005). We use the Bayesian mixed-effects MSORD described here to estimate individual heterogeneity in reproductive rate and individual responses to population growth.

At an individual's first capture f_i she is necessarily a breeder ($z_{i,f_i} = 1$), then switches between breeder ($z_{i,t} = 1$) and nonbreeder ($z_{i,t} = 0$) until her last sighting l_i. To account for confounding effects in estimating individual heterogeneity in reproductive rate, the linear predictor for probability of breeding $\psi^k 1_{i,t}$ also includes standardized population size N_t, a quadratic age effect A, and maternal experience (P, the number of offspring the mother had previously produced). Maternal experience is discretized into 1, 2, 3, and 4+ to account for the nonlinear relationship between female experience and reproductive performance.

For this application, the linear predictor becomes:

$$E[\text{logit}(\psi_{i,t}^{k1})] = \mu_{i,z_{t-1}} + \eta \cdot N_t + \kappa + \pi_1 \cdot A_{i,t} + \pi_2 \cdot A_{i,t}^2 + \alpha_i + \beta_i \cdot N_t + \theta_t$$

where π_1, π_2 are the parameters for the quadratic age effect and κ shifts the intercept μ with maternal experience where $\kappa \in (1,2,3,4)$, and N_t is the estimated population size of the Sable Island breeding herd at time t.

Because this population has been extensively studied, we are able to apply more informed priors to some parameters. Priors for state-specific means μ_0 and μ_1 were given Beta(8,2) priors, reflecting previous analyses that have estimated breeding rates from 80-95%. The standard deviation of the random year effect θ_t was given a Unif(0,5) prior. For the recapture model, we used a

Beta(1,1) prior for entry probability γ, and slightly more informed Beta(6,3) for detection probability $p_{s,t}$ and residence probability ϕ. For components of Σ, a Unif(0,5) prior was specified for random effect variances σ_α and σ_β, and a the correlation among random effects $\rho(\alpha,\beta)$ was given a Unif(-1,1) prior.

Application results & ecological interpretations

We analyzed 200 sighting histories of females that gave birth to 3,132 pups, ranging from 2-26 pups per female with an average of 15.7 pups per female. Ages ranged from 4-33, of which 56.5% (113/200) were seen at the most recent breeding season (2018), and 79.0% (158/200) and 91.5% (183/200) were seen in the last 5, 10 years of the study, respectively.

The model estimated substantial variation among individuals in reproductive rate and in individual responses to population growth, with both parameter posterior distributions distinct from zero (Table 3, Figure 7). The bulk of the posterior distribution and the posterior mean of the correlation among individual effects was positive, though the distribution was not distinct from zero or negative values (Table 3, Figure 8). The positive trend of the ρ posterior indicates that females with high reproductive performance (more positive/greater intercept) were also more likely to respond better to population growth (more positive/greater slope) and vice versa.

The model estimated that individuals that reproduced in year t were more likely to reproduce in year $t+1$ (Table 3, Figure 6), providing no evidence for a cost of reproduction in terms of breeding rate. This result adds to other analyses finding higher breeding probabilities for individuals that bred previously, in grey seals as well as many other taxa (grey seals: den Heyer and Bowen 2017; other taxa: Cam et al. 1998, Hamel et al. 2009, Moyes et al. 2011, Stoelting et al. 2015).

Population size is estimated to have a strong positive effect on reproductive rate (Table 3, Figure 9). This relationship varied among females, with few females showing reduced reproductive performance with increasing population size (individual slope range $\eta+\beta_i$ = [-0.139, 1.132], Table 3, Figure 9). However, as population size is monotonically increasing over the course of this study, the parameter could be capturing variation from other variables with the same trajectory over this period.

Conclusions

In this paper, we have explored the behavior of a Bayesian mixed multistate open-robust design mark recapture model, incorporating individual heterogeneity in both transition rates and response to covariate. We show that the model generally performs well with the most ideal conditions, as specified in our simulation. However, our results underscore recent studies that have also demonstrated the immense data requirements for mark-recapture models. This model is quite "data hungry" and performs relatively poorly with inadequate observations, whether it be in the form of a low sample size, short time series, few secondary samples, and/or low detection rates on the study site, particularly for estimation of individual slopes. With poor estimation of individual slope parameters, estimating the correlation among individual effects $\rho(\alpha, \beta)$ also suffers, yielding relatively uninformed posterior distributions in some simulations. Nevertheless, even in the worst conditions as specified by our simulation, the model-estimated posteriors of vital rates μ_0, μ_1 and the standard deviation among individuals σ_α were well-defined.

While these results lend confidence in estimated parameters for applications such as our grey seal example, with $n = 200$, $T = 30$, and s ranging between 5-7 samples per primary period, and high secondary sample detection rate (estimated as ranging from 0.53 - 0.74, den Heyer et al. 2013), most studies have much smaller scale. Our smallest simulated sample size was 50 individuals observed at 3 sampling sessions per 10 primary periods, which is still considered a large data set for many systems given the realities of collecting data on free-ranging taxa. Further, detection rates at study sites even in the most ideal conditions are typically quite low, which according to our results would make estimation of individual effects (and even the variance of individual effects) quite difficult. Therefore, we caution the use of this model and encourage analysts to perform their own simulations more similar to their dataset before applying our method.

Future Development

Future development of this framework could be used to estimate other important quantities and vital rates in population ecology, such as population size, population growth rate, recruitment, and survival. Similar to (Kendall et al., 2019), this model could be developed to estimate the abundance

of individuals in the reproductive state in a given primary period using a simple Horvitz-Thompson estimator (Horvitz and Thompson 1952). Total abundance, however, is much more difficult due to unobserved states, even ignoring individual variation and assuming purely Markovian transitions (Kendall et al. 2019). So, estimating population size and growth rate may require melding a mixed MSORD and perhaps a data-augmented Jolly-Seber multistate model or POPAN model to estimate a dynamic superpopulation size N with explicitly incorporated individual heterogeneity (den Heyer et al. 2013, Boys et al. 2019).

Our approach modeled individual life histories from their first to last sightings, ignoring recruitment processes and ensuring survival is equal to 1. To estimate survival, a simple step would be to only condition on first capture and incorporate a third, absorbing "dead" state, potentially allowing estimation of cost of reproduction in the form of mortality as transitions to this third state. More difficultly, recruitment parameters require analysts to consider full capture histories such as in the Jolly-Seber model (Jolly 1965, Seber 1965) which has been extended to allow for many different parameterizations of the recruitment process (Crosbie and Manly 1985, Pradel 1996, Link and Barker 2005, Royle 2008). However, future development should consider data requirements and estimability for such expansions of an already data-hungry methodology.

References

Arnason AN. 1972. Parameter estimates from mark-recapture experiments on two populations subject to migration and death. *Researches on Population Ecology* **13**: 97–113. doi: 10.1007/BF02521971.

Beauplet G, Barbraud C, Dabin W, Kussener C, Guinet C, Benton T. 2006. Age-specific survival and reproductive performances in fur seals: Evidence of senescence and individual quality. *Oikos* **112**: 430–441. doi: 10.1111/j.0030-1299.2006.14412.x.

Boulanger J, Cattet M, Nielsen SE, Stenhouse G, Cranston J. 2013. Use of multi-state models to explore relationships between changes in body condition, habitat and survival of grizzly bears Ursus arctos horribilis. *Wildlife Biology* **19**: 274–288. doi: 10.2981/12-088.

Boys RM, Oliveira C, Pérez-Jorge S, Prieto R, Steiner L, Silva MA. 2019. Multi-state open robust design applied to opportunistic data reveals dynamics of wide-ranging taxa: the sperm whale case. *Ecosphere* **10**. doi: 10.1002/ecs2.2610.

Breed GA, Golson EA, Tinker MT. 2016. Predicting animal home-range structure and transitions using a multistate Ornstein-Uhlenbeck biased random walk. *Ecology* **0**: 1–16.

Bull JJ, Shine R. 1979. Iteroparous animals that skip opportunities for reproduction. *American Naturalist* **114**: 296–303.

Cam E, Hines JE, Monnat JY, Nichols JD, Danchin E. 1998. Are adult nonbreeders prudent parents? The kittiwake model. *Ecology* **79**: 2917. doi: 10.2307/176526.

Chambert T, Rotella JJ, Higgs MD, Garrott RA. 2013. Individual heterogeneity in reproductive rates and cost of reproduction in a long-lived vertebrate. *Ecology and Evolution* **3**: 2047–2060. doi: 10.1002/ece3.615.

Crosbie SF, Manly BF. 1985. Parsimonious modelling of capture-mark-recapture studies. *Biometrics* **41**: 385–398.

den Heyer CE, Bowen WD. 2017. Estimating changes in vital rates of Sable Island grey seals using mark-recapture analysis. *Canadian Science Advisory Secretariat Research Document* **2017/054**.

den Heyer CE, Bowen WD, Mcmillan JI. 2013. Long-term changes in grey seal vital rates at Sable Island estimated from POPAN mark-resighting analysis of branded seals. *DFO Canadian Science Advisory Secretariat Research Document* **2013/021**.

Eberhardt LL, Siniff DB. 1977. Population dynamics and marine mammal management policies. *Journal of the Fisheries Research Board of Canada* **34**: 183–190. doi: 10.1139/f77-028.

Frank KT, Petrie B, Choi JS, Leggett WC. 2005. Trophic cascades in a formerly cod-dominated ecosystem. *Science* **308**: 1621–1623. doi: 10.1126/science.1108228.

Gimenez O, Cam E, Gaillard JM. 2017. Individual heterogeneity and capture–recapture models: what, why and how? *Oikos* **127**: 664–686. doi: 10.1111/oik.04532.

Gimenez O, Rossi V, Choquet R, Dehais C, Doris B, Varella H, Vila JP, Pradel R. 2007. State-space modelling of data on marked individuals. *Ecological Modelling* **206**: 431–438. doi: 10.1016/j.ecolmodel.2007.03.040.

Hamel S, Côté SD, Gaillard JM, Festa-Bianchet M. 2009. Individual variation in reproductive costs of reproduction: high quality females always do better. *Journal of Animal Ecology* **78**: 143–151. doi: 10.1111/j.1365-2656.2007.0.

Hernández-Matías A, Real J, Pradel R, Ravayrol A, Vincent-Martin N. 2011. Effects of age, territoriality and breeding on survival of Bonelli's Eagle Aquila fasciata. *Ibis* **153**: 846–857. doi: 10.1111/j.1474-919X.2011.01158.x.

Johns ME, Warzybok P, Bradley RW, Jahncke J, Lindberg M, Breed GA. 2018. Increased reproductive investment associated with greater survival and longevity in Cassin's auklets. *Proceedings of the Royal Society B* **285**. doi: 10.1098/rspb.2018.1464.

Jolly GM. 1965. Explicit estimates from capture-recapture data with both death and immigration-stochastic model. *Biometrika* **52**: 225. doi: 10.2307/2333826.

Kendall WL, Bjorkland R. 2001. Using open robust design models to estimate temporary emigration from capture-recapture data. *Biometrics* **57**: 1113–1122. doi: 10.1111/j.0006-341X.2001.01113.x.

Kendall WL, Nichols JD. 2002. Estimating state-transition probabilities for unobservable states using capture-recapture/resighting data. *Ecology* **83**: 3276–3284. doi: 10.2307/3072078.

Kendall WL, Nichols JD, Hines JE. 1997. Estimating temporary emigration using capture-recapture data with Pollock's robust design. *Ecology* **78**: 563–578. doi: 10.1890/0012-9658(1997)078[0563:ETEUCR]2.0.CO;2.

Kendall WL, Stapleton S, White GC, Richardson JI, Pearson KN, Mason P. 2019. A multistate open robust design: population dynamics, reproductive effort, and phenology of sea turtles from tagging data. *Ecological Monographs* **89**: e01329. doi: 10.1002/ecm.1329.

Kéry M, Schaub M. 2012. *Bayesian Population Analysis using WinBUGS: a hierarchcial perspective*. Elsevier.

Lebreton JD, Almeras T, Pradel R. 1999. Competing events, mixtures of information and multistratum recapture models. *Bird Study* **46**: S39–S46. doi: 10.1080/00063659909477230.

Lebreton JD, Nichols JD, Barker RJ, Pradel R, Spendelow JA. 2009. Modeling individual animal histories with multistate capture-recapture models. In *Advances in Ecological Research*, volume 41. Burlington, VT: Academic Press, 1 edition, 87–173.
URL `http://dx.doi.org/10.1016/S0065-2504(09)00403-6`

Lebreton JD, Pradel R. 2002. Multistate capture recapture models: modelling incomplete individual histories. *Journal of Applied Statistics* **29**: 353–369. doi: 10.1080/02664760120108638.

Link WA, Barker RJ. 2005. Modeling association among demographic parameters in analysis of open population capture-recapture data. *Biometrics* **61**: 46–54. doi: 10.1111/j.0006-341X.2005.030906.x.

McLoughlin PD, Boyce MS, Coulson T, Clutton-Brock T. 2006. Lifetime reproductive success and density-dependent, multi-variable resource selection. *Proceedings of the Royal Society B* **273**: 1449–1454. doi: 10.1098/rspb.2006.3486.

Moyes K, Morgan B, Morris A, Morris S, Clutton-Brock T, Coulson T. 2011. Individual differences in reproductive costs examined using multi-state methods. *Journal of Animal Ecology* **80**: 456–465. doi: 10.1111/j.1365-2656.2010.01789.x.

Pollock KH. 1982. A capture-recapture design robust to unequal probability of capture. *Journal of Wildlife Management* **46**: 752–757. doi: 10.2307/3808568.

Pradel R. 1996. Utilization of capture-mark-recapture for the study of recruitment and population growth rate. *Biometrics* **52**: 703–709.

Rankin RW, Nicholson KE, Allen SJ, Krützen M, Bejder L, Pollock KH. 2016. A full-capture Hierarchical Bayesian model of Pollock's Closed Robust Design and application to dolphins. *Frontiers in Marine Science* **3**: 1–18. doi: 10.3389/fmars.2016.00025.

Riecke TV, Sedinger BS, Williams PJ, Leach AG, Sedinger JS. 2019. Estimating correlations among demographic parameters in population models. *Ecology and Evolution* **9**: 13521–13531. doi: 10.1002/ece3.5809.

Royle JA. 2008. Modeling individual effects in the Cormack-Jolly-Seber model: A state-space formulation. *Biometrics* **64**: 364–370. doi: 10.1111/j.1541-0420.2007.00891.x.

Schwarz CJ, Stobo WT. 1997. Estimating temporary migration using the robust design. *Biometrics* **53**: 178–194. doi: 10.2307/2533106.

Seber GAF. 1965. Note on the multiple-recapture census. *Biometrika* **52**: 249. doi: 10.2307/2333827.

Stoelting RE, Gutiérrez RJ, Kendall WL, Peery MZ. 2015. Life-history tradeoffs and reproductive cycles in Spotted Owls. *The Auk* **132**: 46–64. doi: 10.1642/auk-14-98.1.

Zachar N, Neiman M. 2013. Profound effects of population density on fitness-related traits in an invasive freshwater snail. *PLoS ONE* **8**. doi: 10.1371/journal.pone.0080067.

Tables

Table 1: Listed 32 sets of conditions in simulated datasets. In this analysis, the set of conditions (simulation) in each row is replicated 50 times, for a total of 1600 model fits. n is sample size, T is the number of primary periods over the course of the study, s is the number of secondary observation periods per primary period, h is the standard deviation among individuals in individual effects, and p is the detection rate during secondary periods.

Simulation	n	T	h	s	p
1	100	20	7	0.1	0.7
2	50	20	7	0.1	0.7
3	100	10	7	0.1	0.7
4	100	20	3	0.1	0.7
5	100	20	7	0.5	0.7
6	100	20	7	0.1	0.3
7	50	10	7	0.1	0.7
8	50	20	3	0.1	0.7
9	50	20	7	0.5	0.7
10	50	20	7	0.1	0.3
11	100	10	3	0.1	0.7
12	100	10	7	0.5	0.7
13	100	10	7	0.1	0.3
14	100	20	3	0.5	0.7
15	100	20	3	0.1	0.3
16	100	20	7	0.5	0.3
17	50	10	3	0.1	0.7
18	50	10	7	0.5	0.7
19	50	10	7	0.1	0.3
20	50	20	3	0.5	0.7
21	50	20	3	0.1	0.3
22	50	20	7	0.5	0.3
23	100	10	3	0.5	0.7
24	100	10	3	0.1	0.3
25	100	10	7	0.5	0.3
26	100	20	3	0.5	0.3
27	50	10	3	0.5	0.7
28	50	10	3	0.1	0.3
29	50	10	7	0.5	0.3
30	50	20	3	0.5	0.3
31	100	10	3	0.5	0.3
32	50	10	3	0.5	0.3

Table 2: Proportion of replicates from each simulation with $\hat{r} < 1.1$, for each parameter.

Simulation	μ^{11}	μ^{01}	σ_α	σ_β	$\rho(\alpha, \beta)$
1	1.0	1.0	1.0	1.0	1.0
2	1.0	1.0	1.0	1.0	1.0
3	1.0	1.0	0.8	1.0	1.0
4	1.0	1.0	0.8	0.8	1.0
5	1.0	1.0	1.0	1.0	1.0
6	1.0	1.0	1.0	0.8	1.0
7	1.0	0.8	1.0	1.0	1.0
8	1.0	1.0	1.0	1.0	1.0
9	1.0	1.0	1.0	1.0	1.0
10	1.0	1.0	1.0	1.0	1.0
11	1.0	0.8	0.8	0.4	1.0
12	1.0	1.0	1.0	0.2	0.8
13	11.0	1.0	1.0	0.6	1.0
14	1.0	1.0	1.0	1.0	1.0
15	1.0	1.0	1.0	1.0	1.0
16	1.0	1.0	1.0	1.0	1.0
17	1.0	1.0	0.8	0.6	1.0
18	1.0	1.0	1.0	0.6	1.0
19	1.0	1.0	1.0	1.0	1.0
20	1.0	1.0	1.0	0.8	1.0
21	1.0	1.0	1.0	1.0	1.0
22	1.0	1.0	1.0	1.0	1.0
23	1.0	1.0	0.6	0.6	1.0
24	1.0	1.0	0.6	0.4	1.0
25	1.0	0.8	1.0	0.6	1.0
26	1.0	1.0	1.0	1.0	1.0
27	1.0	1.0	0.8	0.8	1.0
28	1.0	1.0	0.6	0.4	1.0
29	1.0	1.0	1.0	0.4	1.0
30	1.0	1.0	1.0	1.0	1.0
31	1.0	0.8	0.4	0.8	1.0
32	1.0	1.0	1.0	1.0	1.0
Average:	1.0	0.88	0.71	0.50	0.99

Table 3: Parameter estimates for application to grey seal reproductive heterogeneity, including means, modes, standard deviation (SD), 95% credible interval (CRI) and 95% highest posterior density (HPD). μ represents reproductive rate (probability of being in breeding state $z_{i,t} = 1$) with the subscript defining their state in year t-1 (1 = breeding, 0 = not breeding). σ is the variance of the distribution describing the random effect specified in the subscript; and ρ estimates the correlation of the random effects listed in the parentheses. η describes the population-level (i.e. fixed) effect of the breeding herd size N_t.

Parameter	Mean	Mode	SD	CRI	HPD
μ_1	0.891	0.911	0.055	[0.754, 0.961]	[0.799, 0.981]
μ_0	0.747	0.776	0.103	[0.507, 0.909]	[0.551, 0.933]
σ_α	1.065	1.055	0.151	[0.796, 1.358]	[0.787, 1.343]
σ_β	0.629	0.633	0.186	[0.292, 1.030]	[0.237, 0.961]
$\rho(\sigma_\alpha, \sigma_\beta)$	0.307	0.489	0.339	[-0.408, 0.869]	[-0.357, 0.886]
η	0.522	0.530	0.097	[0.333, 0.699]	[0.332, 0.699]

Figures

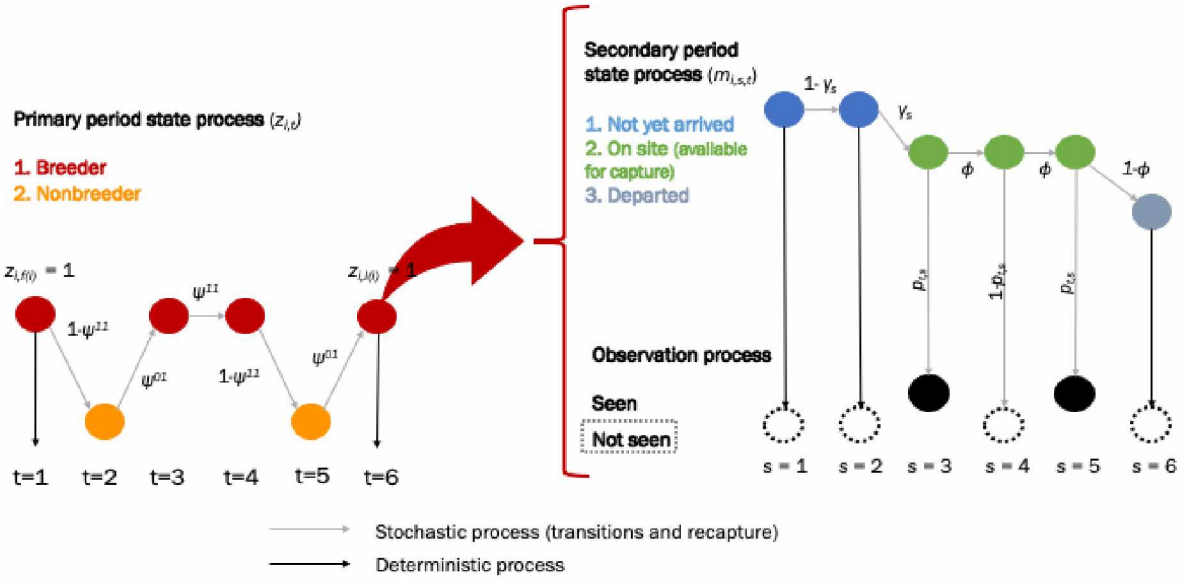

Figure 1: Conceptual diagram of mutlistate robust design mark-recapture model process (modified from Kéry and Schaub 2012). Observations of the secondary state process (left) informs the primary period state process z (right) through a series of stochastic and deterministic transitions and observations. At her first primary occasion $(z_i, f(i))$, the female is necessarily in a breeding state, and is thus available for capture. In secondary occasions $s \in \{1, 2, \ldots, S\}$ she moves through a series of states: not yet arrived at study area, at study area, and departed from the study area. Based on observations from this period, the model estimates the sequence of primary states (breeder, nonbreeder) over a female's capture history.

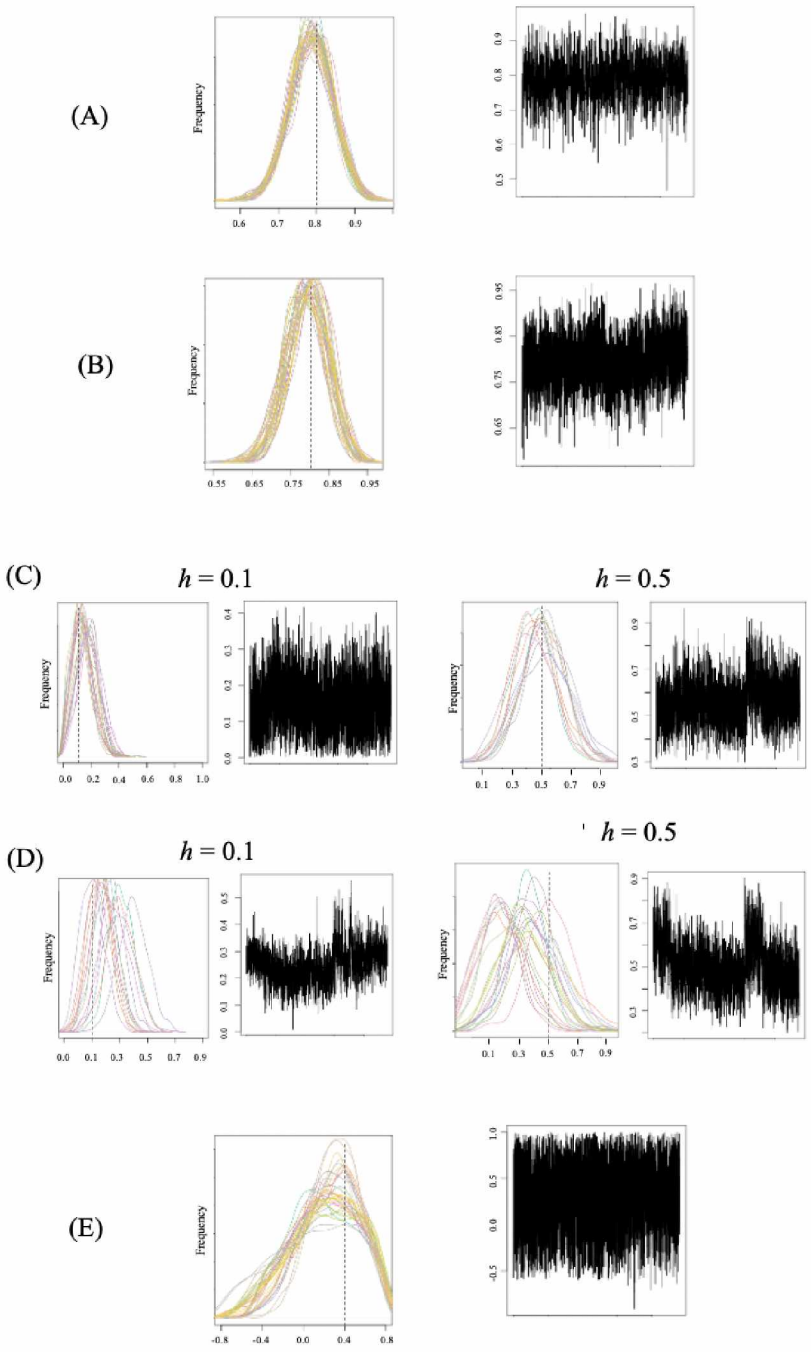

Figure 2: Hierarchical posterior distributions (lines) and example traceplot for each parameter. Vertical dashed lines mark simulated true value. (A) is μ_1, (B) is μ_0, (C) is σ_α with L and R panels depicting models with $h = 0.1$ and $h = 0.5$ respectively, (D) is σ_β with L and R panels depicting models with $h = 0.1$ and $h = 0.5$ respectively, and (E) is $\rho(\alpha, \beta)$.

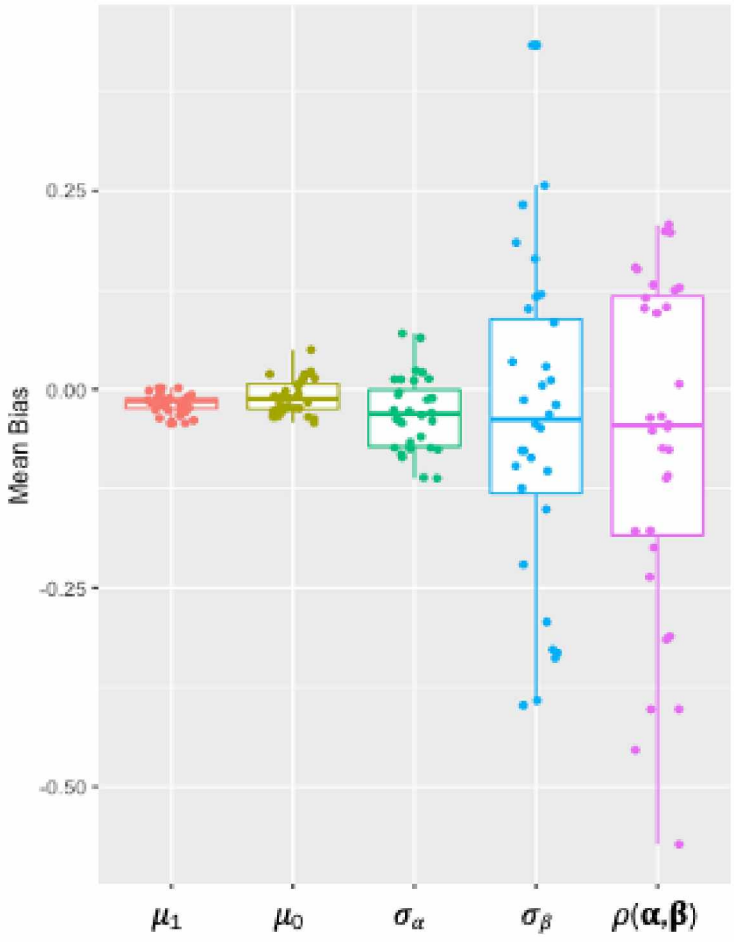

Figure 3: Bias in posterior mean across hierarchical model fits for each parameter.

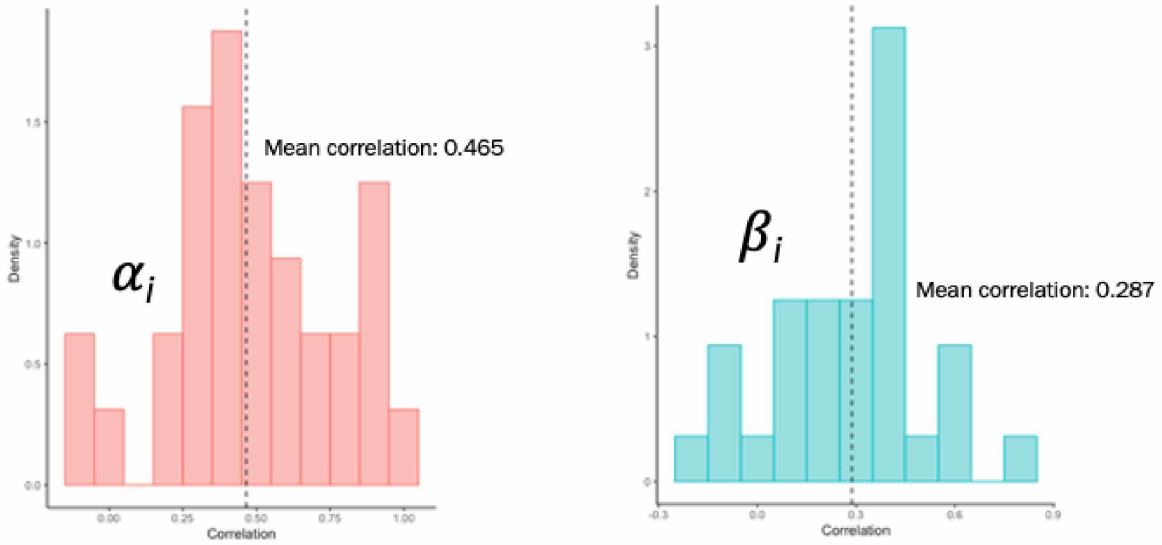

Figure 4: Histogram of correlation between true values and hierarchical posterior means of individual effects α (red) and β (blue) for the 32 hierarchical model fits.

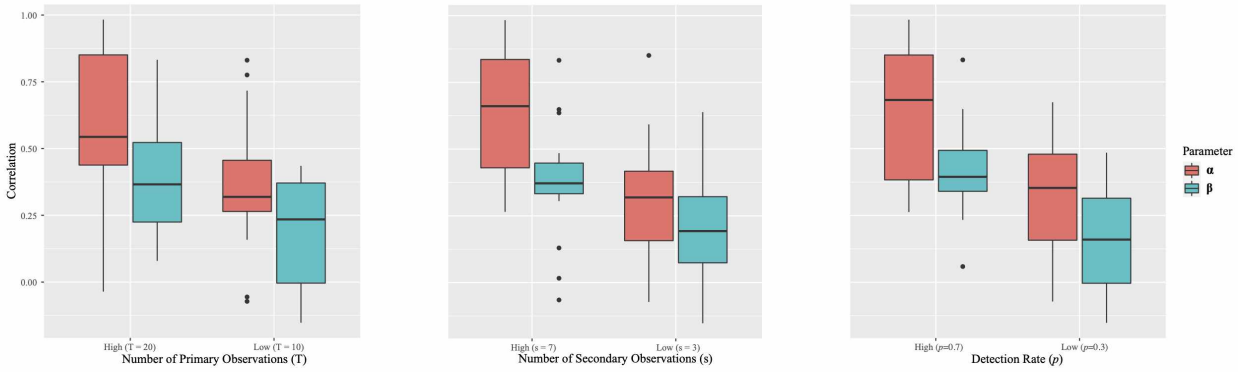

Figure 5: Correlation between estimated hierarchical posterior mean of individual effects α and β and their true value, as influenced by length of time series (T), number of secondary periods (s), and detection probability (p).

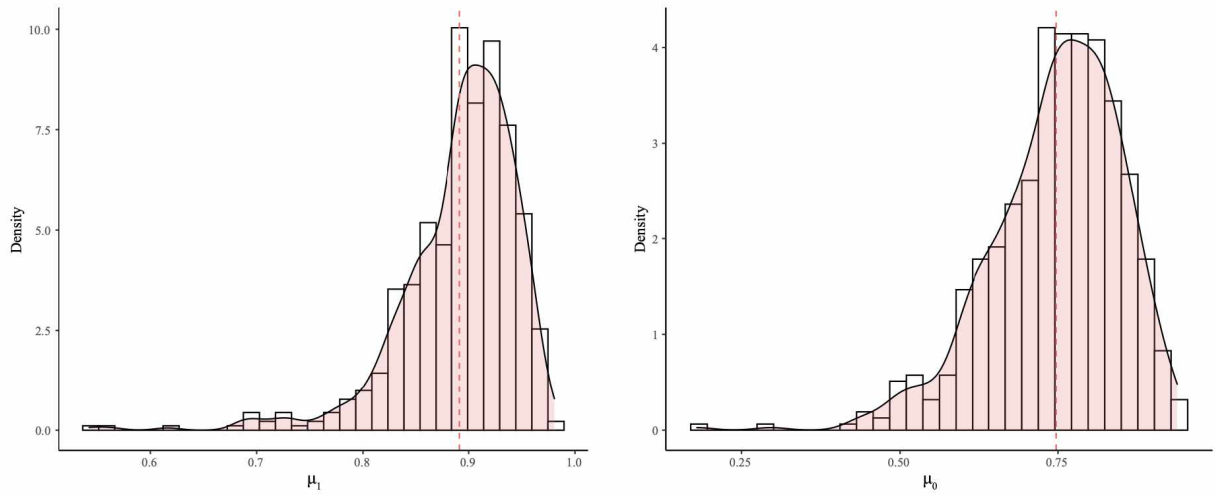

Figure 6: Posterior distributions of the mean probability of breeding for individuals that (A) bred previously (μ_1) and (B) skipped breeding in the previous year (μ_0) for our application of the Bayesian mixed MSORD to the sample of grey seal females.

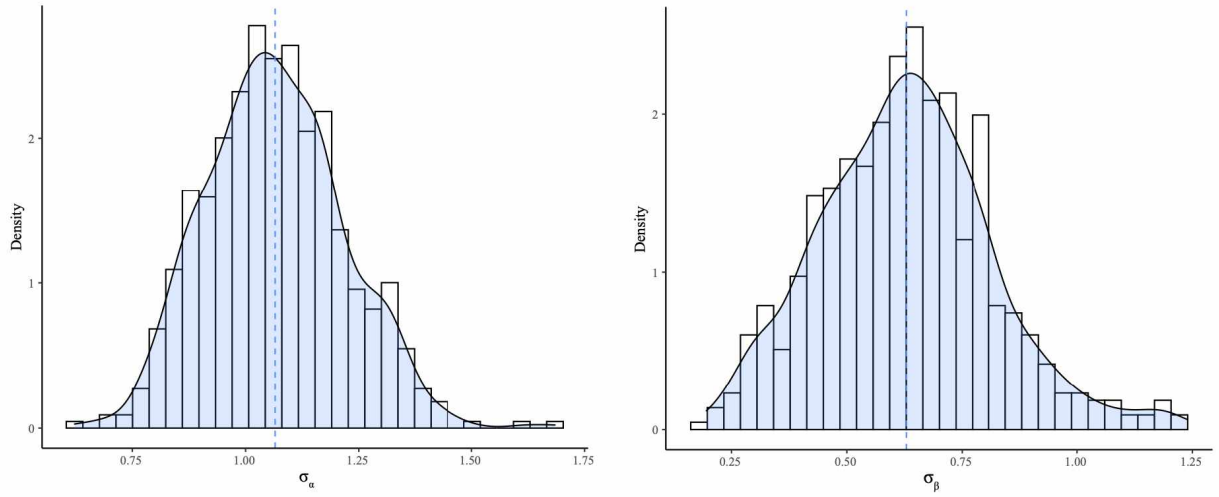

Figure 7: Posterior distributions of the variation among individuals in (A) intercepts (σ_α) and (B) slopes with estimated population size (σ_β) for our application of the Bayesian mixed MSORD to the sample of grey seal females.

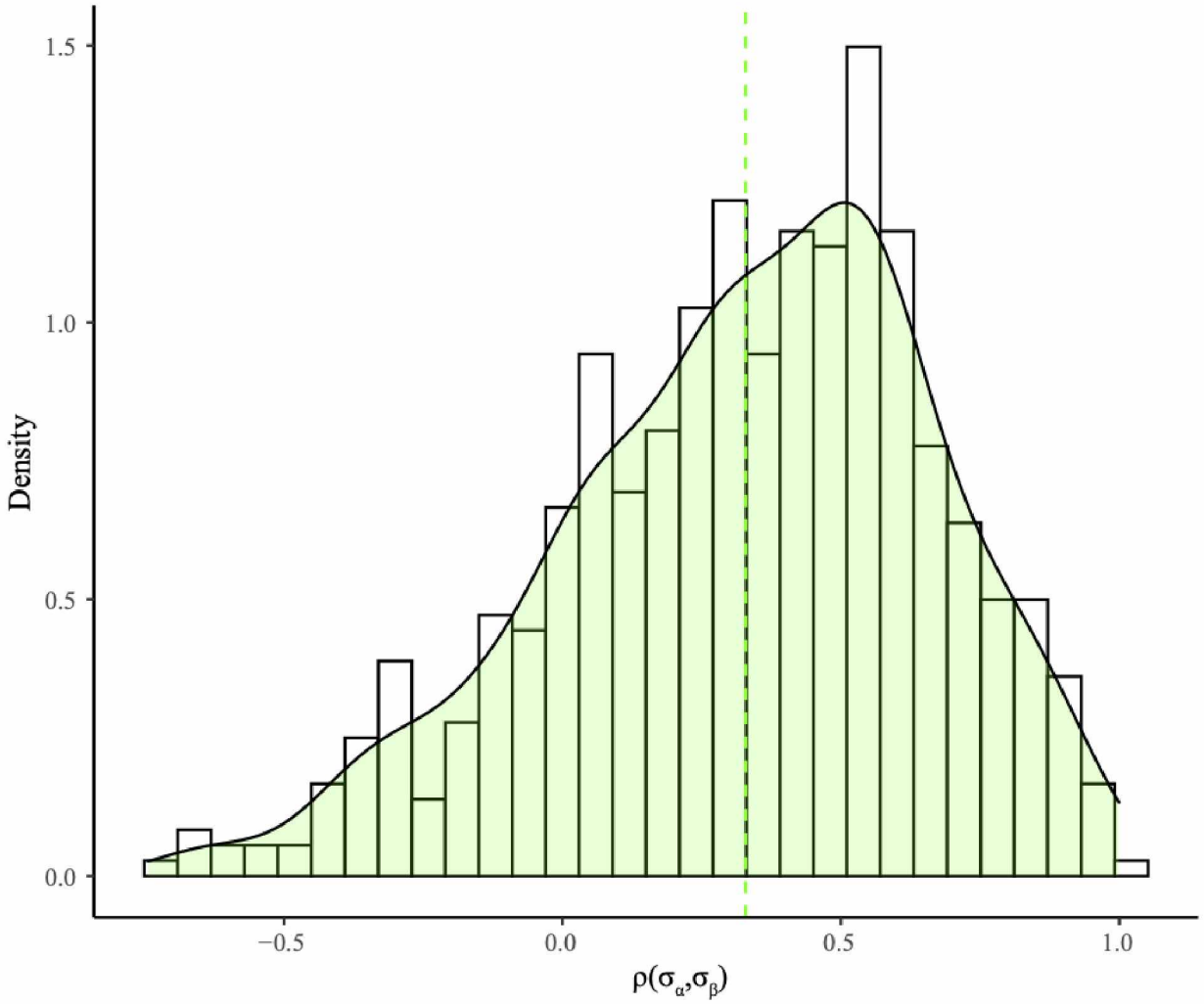

Figure 8: Estimated correlation between estimated individual effects α and β for our application of the Bayesian mixed MSORD to the sample of grey seal females.

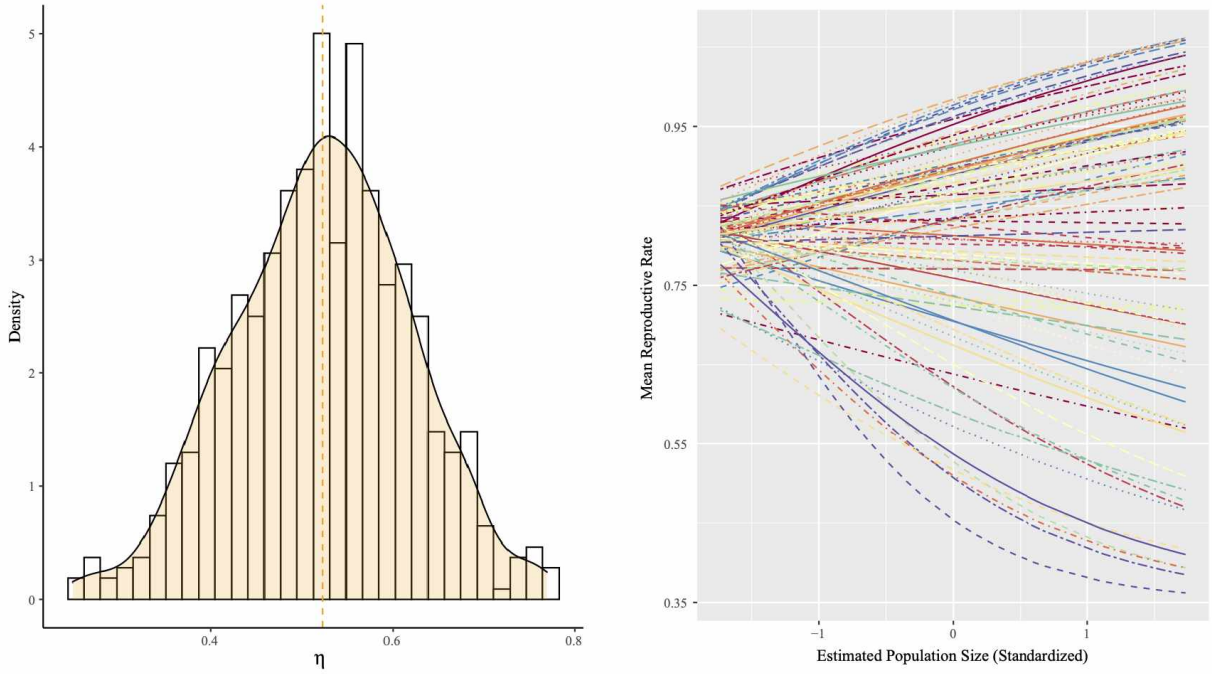

Figure 9: The estimated effect of population size on reproductive rate of female grey seals: (A) posterior distribution of parameter describing the effect of population size on grey seal reproductive rate, η, and (B) estimated reproductive rate over increasing population sizes, with each line representing the trajectory for individual i, calculated form the posterior means of α_i, β_i, μ_1, and η from a sample of 75 females in the dataset.